Electrophoresis of Spheres by a Discretized Integral Equation/ Finite Difference Approach

Stuart A. Allison* and P. Nambi

Department of Chemistry, Georgia State University, Atlanta, Georgia 30303

*Received August 11, 1993; Revised Manuscript Received December 7, 1993**

ABSTRACT: A numerical algorithm is developed to study the electrophoresis of polyions where account is taken of ionic relaxation. The algorithm involves simultaneous solution of the Navier–Stokes equation by a discretized integral equation method and of Poisson and ion-transport equations by the finite difference method. It is applied to the electrophoresis of spherical polyions containing centrosymmetric charges, and the resulting mobilities are in excellent agreement with those of Wiersema et al. (*J. Colloid Interface Sci.* **1966,** *22,* 78). The extent to which ion relaxation perturbs the charge density and velocity field around the polyion is investigated.

I. Introduction

In the solvent environment near charged macromolecules such as colloids, proteins, certain synthetic polypeptides, and nucleic acids, large but localized electrostatic potentials can exist which significantly alter the local ionic environment from that found in the bulk solution. External forces on the solvent can be large in the vicinity of polyions, and these forces alter the pressure and velocity fields around them and hence their transport properties. Recently, a numerical method was developed which accounts for the effects of steady-state external forces on the solvent.[1] It is based on the integral equations of the Stokes equations which date back to Lorentz[2] and subsequent work by Odqvist.[3] Ladyshenskaya[4] summarized the integral equation theory in a now popular text. Youngren and Acrivos were the first to implement this approach numerically by applying it to cases where external solvent forces were ignored.[5,6] This was achieved by reducing the integral equations to a system of linear algebraic equations which shall be referred to in the remainder of this work as the discretized integral equation (DIE) method. In ref 1, external forces were incorporated into the DIE approach and it was applied to the problem of a charged spherical polyion in which relaxation of the ion atmosphere away from its equilibrium distribution was ignored. The results were found to be in good agreement with the theory of Henry.[7]

A number of investigators have studied the effect of ion relaxation on the electrophoretic mobility of charged spheres (centrosymmetrically distributed) in solution.[8–12] Whether or not its inclusion is important depends on the size of the spherical polyion, its net charge or surface (ζ) potential, the solvent, and the nature of the co-ions and counterions present. It will prove convenient to define a reduced surface potential, $y_0 = q\zeta/k_BT$, where q is the protonic charge, k_B is Boltzmann's constant, and T is the absolute temperature. For an aqueous monovalent salt solution at room temperature with $\kappa a = 5$ (κ is the Debye–Hückel screening parameter and a the sphere radius) and ionic mobilities comparable to those of Na^+ and Cl^+ ions, ionic relaxation will significantly affect the electrophoretic mobility if y_0 exceeds about 1.5.[10,11] These conditions are met, for example, if $a = 2.0$ nm, the salt concentration is 0.576 M, and the net charge of the polyion exceeds about $\pm 27q$.

Ion relaxation may not be particularly important for most proteins since net charges rarely exceed this value. It is, however, important for many colloids.[11] Although this treatment is strictly valid for spherical polyions, we may also expect it to be qualitatively correct for rodlike polyions as well. Since the reduced potential of DNA is estimated to be between about 1.5 and 3.5,[13] ion relaxation is probably significant in that important case.

The primary objective of this work is to extend the DIE method to include ionic relaxation. In the absence of relaxation, what is basically required is a numerical solution of the Navier–Stokes equation at low Reynolds number to determine the pressure and fluid velocity fields around a polyion modeled as a rigid object. The external forces on the solvent are derived from the electrostatic potential and ionic charge distributions which, in turn, are derived from the solution of the Poisson–Boltzmann equation. For a spherical polyion, these are well-known.[1,14] When ion relaxation is included, we need to know how the external field perturbs the ion atmosphere from its equilibrium distribution. In addition to solving the Navier–Stokes equation, the Poisson and ion-transport equations have to be solved simultaneously as well. Wiersema and coworkers[10,11] and also O'Brien and White[12] have developed numerical algorithms to accomplish this. Here, a somewhat different numerical approach is developed in which the technique of finite differences is used to solve the Poisson and ion-transport equations. The method of finite differences has been very successful in solving the Poisson–Boltzmann equation around complex models of charged macromolecules.[15–20] The results of these calculations have been used in detailed modeling studies of diffusion-controlled reactions,[21,22] shifts in pK values of protein residues,[23] and the determination of electrostatic forces on solvated molecules.[24] It is hoped that the algorithm developed here of simultaneously solving the Navier–Stokes equation (by the DIE approach) and the Poisson and ion-transport equations (by finite differences) will ultimately be useful in studying the transport of rigid macromolecules of arbitrary shape.

In order to test the algorithm and determine which features are important in obtaining accurate electrophoretic mobilities, we shall restrict ourselves to spherical polyions which contain centrosymmetric charge distributions. In addition to electrophoretic mobilities, we will examine how the ion atmosphere is perturbed in the vicinity of the polyion and how this is influenced by the dielectric constant of the polyion interior. We will end by

* Abstract published in *Advance ACS Abstracts,* February 15, 1994.

0024-9297/94/2227-1413$04.50/0

discussing some of the difficulties of extending this work to more complex problems.

II. Determination of the Electrophoretic Mobility

The calculation of the electrophoretic mobility of a polyion requires detailed knowledge of the hydrodynamic and electrostatic forces which act on it. The polyion shall be modeled as a solid rigid body enclosed by a surface S_p characterized by an interior dielectric constant, ϵ_1. The surrounding fluid is treated as a continuous incompressible liquid (with the dielectric constant equal to ϵ_2) that satisfies the Navier–Stokes equation. At low Reynolds number, the Navier–Stokes and solvent incompressibility equations can be written:

$$\eta\nabla^2\mathbf{v}(\mathbf{x}) - \nabla p(\mathbf{x}) = -\mathbf{s}(\mathbf{x}) \qquad \mathbf{x} \in \Omega \tag{1}$$

$$\nabla\cdot\mathbf{v}(\mathbf{x}) = 0$$

where η is the solvent viscosity, $p(\mathbf{x})$ is the pressure at $\mathbf{x}$ ($\mathbf{x}$ is in the domain occupied by the fluid which is designated by Ω), and $\mathbf{s}(\mathbf{x})$ is the force per unit volume on the fluid at $\mathbf{x}$ due to external forces. $p(\mathbf{x})$ and $\mathbf{v}(\mathbf{x})$ can be solved by a discretized integral equation (DIE) method.[1,5,6] The first part of the appendix outlines this method for the general case, and the latter part treats a spherical polyion with a centrosymmetric charge distribution. For now, it is sufficient to point out that the DIE approach enables one to calculate $\mathbf{v}(\mathbf{x})$ and $p(\mathbf{x})$ for an arbitrary rigid polyion as well as the surface stress forces, $\mathbf{f}(\mathbf{y})$, acting on the fluid due to the polyion at surface point $\mathbf{y}$.

$$\mathbf{f}(\mathbf{y}) = (\lim_{x\to y} \mathbf{T}_h(\mathbf{x}))\cdot\mathbf{n}(\mathbf{y}) \tag{2}$$

where $\mathbf{T}_h$ is the hydrodynamic stress tensor,

$$(\mathbf{T}_h(\mathbf{x}))_{ij} = -p(\mathbf{x})\,\delta_{ij} + \eta\left(\frac{\partial v_i(\mathbf{x})}{\partial x_j} + \frac{\partial v_j(\mathbf{x})}{\partial x_i}\right) \tag{3}$$

$\mathbf{n}(\mathbf{y})$ denotes the inward unit normal to the particle surface at $\mathbf{y}$, and δ_{ij} is the Kronecker delta. The total hydrodynamic force on the polyion can be written as

$$\mathbf{z}_h = -\int_{S_p} \mathbf{f}(\mathbf{y})\,dS_y \simeq -\sum_j \mathbf{f}_j A_j \tag{4}$$

where the second equality comes from the approximation of breaking up the surface of the polyion into patches of area A_j and assuming the stress forces are constant over a given patch. This is the essence of the DIE algorithm. There is also an electrostatic force, $\mathbf{z}_e$, on the polyion which can be written

$$\mathbf{z}_e = -\int_{S_p} \mathbf{T}_e(\mathbf{y})\cdot\mathbf{n}(\mathbf{y})\,dS_y \tag{5}$$

where $\mathbf{T}_e$ is the Maxwell stress tensor[25]

$$\mathbf{T}_e(\mathbf{y}) = \frac{\epsilon_2}{4\pi}\left[\mathbf{E}(\mathbf{y}) - \frac{1}{2}(\mathbf{e}(\mathbf{y})\cdot\mathbf{e}(\mathbf{y}))\mathbf{I}\right] \tag{6}$$

$\mathbf{e}$ is the electric field and $\mathbf{E}_{ij} = (\mathbf{e})_i(\mathbf{e})_j$ is the electric field dyadic. The total force on the polyion, $\mathbf{z}_t$, is simply the sum.

$$\mathbf{z}_t = \mathbf{z}_h + \mathbf{z}_e = -\int_{S_p} (\mathbf{T}_h(\mathbf{y}) + \mathbf{T}_s(\mathbf{y}))\cdot\mathbf{n}\,dS_y \tag{7}$$

In the special case of a polyion in the absence of flow ($\mathbf{v}(\mathbf{x}) = 0$) and absence of relaxation of the ion atmosphere (charge density unperturbed from its equilibrium distribution), eq 7 becomes

$$\mathbf{z}_t^0 = -\int (-p_0(\mathbf{y})\,\mathbf{I} + \mathbf{T}_e(\mathbf{y}))\cdot\mathbf{n}\,dS_y \tag{8}$$

where $p_0(\mathbf{y})$ is the osmotic pressure at the polyion surface. Recently, there has been considerable interest in calculating electrostatic forces on solvated molecules. Equation 8 above reduces to eq 15 of Gilson et al. in the linear Poisson–Boltzmann approximation.[24] In the present analysis, however, the osmotic pressure term is labeled as a hydrodynamic rather than electrostatic component.

In order to determine the electrophoretic mobility of a polyion, one must determine the translational velocity, $-\mathbf{u}$, of the polyion placed in a constant electric field, $-\mathbf{e}_0$, which gives $\mathbf{z}_t = \mathbf{0}$. In this work, the rotational motion of the polyion shall be ignored. This is done following O'Brien and White.[12] For external fields small compared to the fields near the polyion, $\mathbf{z}_t$ will vary linearly with u and $\mathbf{e}_0$. Also, for the simple geometries considered in the present work, $\mathbf{z}_t$, $\mathbf{u}$, and $\mathbf{e}_0$ will be collinear. First, translate the polyion with velocity $-\mathbf{u}_0$ in the absence of the electric field and denote the net force $\mathbf{z}_t^{(1)} = \alpha\mathbf{u}_0$. Next, hold the polyion stationary in an external field $-\mathbf{e}_0$ and determine $\mathbf{z}_t^{(2)} = \beta\mathbf{e}_0$. The resulting mobility is then simply

$$u/e_0 = -\beta/\alpha \tag{9}$$

We shall be reporting reduced mobilities, μ_{red}, defined by

$$\mu_{red} = \left(\frac{6\pi\eta q}{\epsilon_2 k_B T}\right)\left(\frac{u}{e_0}\right) \tag{10}$$

where η is the solvent viscosity (taken to be 0.89 cP), q(=4.8 × 10^{-10} esu) is the protonic charge, k_B is Boltzmann's constant, and T is the absolute temperature (taken to be 298.15 K).

We shall assume the system satisfies the Poisson

$$\nabla\cdot(\epsilon(\mathbf{x})\,\nabla\Lambda(\mathbf{x})) = -4\pi\rho(\mathbf{x}) \tag{11}$$

$$\rho(\mathbf{x}) = q\lambda\sum_\alpha z_\alpha n_\alpha(\mathbf{x}) + \rho_f(\mathbf{x}) \tag{12}$$

and ion transport ($\mathbf{x} \in \Omega$)

$$\nabla\cdot(n_\alpha(\mathbf{x})\,\mathbf{v}_\alpha(\mathbf{x})) = 0 \tag{13}$$

equations where Λ is the electrostatic potential, ρ the net charge density, ρ_f is the fixed charge density associated with the polyion, and λ is a screening function equal to zero inside the polyion and equal to 1 for $\mathbf{x} \in \Omega$; n_α, z_α, and $\mathbf{v}_\alpha$ are the concentration, valency, and mean velocity of ion species α. The ion velocity can be written as

$$\mathbf{v}_\alpha(\mathbf{x}) = \mathbf{v}(\mathbf{x}) - \frac{z_\alpha q}{k_B T}D_\alpha\nabla\Lambda(\mathbf{x}) - D_\alpha\nabla(\ln n_\alpha(\mathbf{x})) \tag{14}$$

where D_α is the diffusion constant of α. For a polyion translating with velocity $-\mathbf{u}$ and stick boundary conditions, we must have

$$\mathbf{v}_\alpha(\mathbf{x})\cdot\mathbf{n} = -\mathbf{u}\cdot\mathbf{n} \tag{15}$$

at the polyion surface. Introduce the reduced potential, $y = q\Lambda/k_B T$, along with the perturbations in n_α and y from their equilibrium values, $n_{\alpha 0}$ and y_0

$$n_\alpha = n_{\alpha 0} + \delta n_\alpha$$

$$y = y_0 + \delta y \tag{16}$$

where the dependence on $\mathbf{x}$ has been omitted for brevity. Equations 11 and 12 become

$$\nabla\cdot(\epsilon\nabla y_0) = -\frac{4\pi q^2\lambda}{k_BT}\sum_\alpha z_\alpha n_\alpha^0 - \frac{4\pi q\rho_f}{k_BT} \tag{17}$$

$$\nabla\cdot(\epsilon\nabla\,\delta y) = -\frac{4\pi q^2\lambda}{k_BT}\sum_\alpha z_\alpha\,\delta n_\alpha \tag{18}$$

where eq 17 is just the Poisson–Boltzmann equation and eq 18 relates the perturbation potential, δy, to the perturbation in ion concentrations. To lowest order in $\mathbf{v}$, δy, and δn_α, eq 14 becomes

$$\mathbf{v}_\alpha = \mathbf{v} - D_\alpha[z_\alpha\nabla\,\delta y + \nabla(n_{\alpha0}^{-1}\,\delta n_\alpha)] \tag{19}$$

Following O'Brien and White,[12] introduce the reduced potential $\phi_\alpha(\mathbf{x})$ defined by

$$\begin{aligned} n_\alpha &= n_{\alpha0}e^{-z_\alpha(\delta y+\phi_\alpha+\mathbf{b}\cdot\mathbf{r})} \\ &= n_{\alpha0}(1 - z_\alpha(\delta y + \phi_\alpha + \mathbf{b}\cdot\mathbf{r})) \end{aligned} \tag{20}$$

where $\mathbf{b} = -q\mathbf{e}_0/k_BT$ is a reduced external field. The ion velocity can be written

$$\mathbf{v}_\alpha = \mathbf{v} + D_\alpha z_\alpha(\nabla\phi_\alpha + \mathbf{b}) \tag{21}$$

and the boundary condition on the polyion surface (eq 15) yields $\nabla\phi_\alpha = -\mathbf{b}$.

In terms of the potential ϕ_α eqs 13 and 18 become

$$0 = \nabla\cdot\mathbf{v} + D_\alpha z_\alpha\nabla^2\phi_\alpha - z_\alpha[\mathbf{v} + D_\alpha z_\alpha(\nabla\phi_\alpha + \mathbf{b})]\cdot\nabla y_0 \tag{22}$$

$$\nabla\cdot(\epsilon\nabla\,\delta y) = \frac{4\pi q^2\lambda}{k_BT}\sum_\alpha n_{\alpha0}z_\alpha^2[\delta y + \phi_\alpha + \mathbf{b}\cdot\mathbf{x}] \tag{23}$$

The velocity field $\mathbf{v}$ depends on ϕ_α and δy through the external forces which, for the system of interest here, can be written as

$$\mathbf{s} = -\rho\nabla\Lambda \tag{24}$$

The problem will be solved by successive iteration. To get an initial estimate of $\mathbf{v}$, call it $\mathbf{v}^{(1)}$, ignore completely the relaxation of the ion atmosphere. Then

$$\mathbf{s}^{(1)} = -\rho_0\nabla\Lambda^{(1)} \tag{25}$$

where

$$\Lambda^{(1)} = \frac{k_BT}{q}(y_0 + \delta y^{(1)}) \tag{26}$$

and $\delta y^{(1)}$ is the correction potential in the absence of relaxation. Since $\delta n_\alpha = 0$ in this case we must have from eq 20

$$\phi_\alpha^{(1)} = -\delta y^{(1)} - \mathbf{b}\cdot\mathbf{x} \tag{27}$$

In general, $\delta y^{(1)}$ will be the solution of eq 23 with the right-hand side set equal to zero subject to the boundary condition at infinity $\delta y^{(1)} = -\mathbf{b}\cdot\mathbf{x}$. For a sphere of radius a with interior/exterior dielectric constants of ϵ_1/ϵ_2

$$\delta y^{(1)} = -\mathbf{b}\cdot\mathbf{x}[1 + (\epsilon_2 - \epsilon_1)a^3/((2\epsilon_2 + \epsilon_1)x^3)] \tag{28}$$

which represents the electrostatic potential due to a constant external field (equal to $-\mathbf{e}_0 = k_BT\mathbf{b}/q$) plus the reaction field of a dielectric sphere. The velocity field, $\mathbf{v}^{(1)}$, is then solved following the procedure described in the appendix.

We are now in a position to solve for $\phi_\alpha^{(2)}$ and $\delta y^{(2)}$. Since the same scheme is used in later iteration cycles, replace suffixes 1 and 2 with i and $i+1$. Equation 22 is first solved to obtain updated ϕ_α's ($\phi_\alpha^{(i+1)}$)

$$\begin{aligned} 0 = \nabla\cdot\mathbf{v}^{(i)} + D_\alpha z_\alpha\nabla^2\phi_\alpha^{(i+1)} - \\ z_\alpha[\mathbf{v}^{(i)} + D_\alpha z_\alpha(\nabla\phi_\alpha^{(i+1)} + \mathbf{b})]\cdot\nabla y_0 \end{aligned} \tag{29}$$

Then updated reduced potentials, $y^{(i+1)}$, are obtained by solving

$$\begin{aligned} \nabla\cdot(\epsilon\nabla(y^{(i+1)} - y^{(i)})) = \\ \frac{4\pi q^2\lambda}{k_BT}\sum_\alpha n_{\alpha0}z_\alpha^2[y^{(i+1)} - y^{(i)} + \phi_\alpha^{(i+1)} - \phi_\alpha^{(i)}] \end{aligned} \tag{30}$$

Equations 29 and 30 are relevant to any rigid polyion and must be solved to account for ionic relaxation. In what follows, we shall restrict ourselves to a spherical polyion. The reader not greatly interested in the mathematical details may skip the next section.

III. Spherical Polyion with Centrosymmetric Charge Distribution

For a sphere, the velocity field can be written (omitting the superscript).

$$\begin{aligned} \mathbf{v}(r,\theta) &= v_r(r,\theta)\,\mathbf{e}_r + v_\theta(r,\theta)\,\mathbf{e}_\theta \\ &= v_1(r)\cos\theta\mathbf{e}_r + v_2(r)\sin\theta\mathbf{e}_\theta \end{aligned} \tag{31}$$

where

$$\begin{aligned} \mathbf{e}_r &= \mathbf{i}\cos\theta + \mathbf{j}\sin\theta\cos\phi + \mathbf{k}\sin\theta\sin\phi \\ \mathbf{e}_\theta &= -\mathbf{i}\sin\theta + \mathbf{j}\cos\theta\cos\phi + \mathbf{k}\cos\theta\sin\phi \end{aligned} \tag{32}$$

The flow direction is taken along the x axis. By calculating the velocity fields at a series of points along the x and y axes, we can interpolate $\mathbf{v}(r,\theta)$ at all points. For $\theta = 0$, $\mathbf{v}(r,0) = \mathbf{i}v_1(r)$ and for $\theta = \pi/2$, $\mathbf{v}(r,\pi/2) = -\mathbf{i}v_2(r)$.

It is also possible to convert eqs 29 and 30 from three to one dimensions for a sphere. Introduce the new variables

$$\phi_\alpha^{(i)}(r,\theta) = g_\alpha^{(i)}(r)\cos\theta \tag{33}$$

$$b_r(\theta) = b\cos\theta \tag{34}$$

$$y^{(i+1)}(r,\theta) - y^{(i)}(r,\theta) = f^{(i+1)}(r)\cos\theta \tag{35}$$

Equation 29 is then integrated over a small volume extending from $r_j - \delta r/2$ to $r_j + \delta r/2$ and from $\theta = 0$ to $\theta = \delta\theta$ where $\delta\theta$ is taken to be very small. The result is

$$\begin{aligned} 0 = (\nabla\cdot\mathbf{v}^{(i)})_j + D_\alpha z_\alpha\Bigg[\left(1 + \frac{\delta r^2}{4r_j^2}\right)(g_{\alpha j+1}^{(i+1)} - 2g_{\alpha j}^{(i+1)} + \\ g_{\alpha j-1}^{(i+1)})/\delta r^2 + \left(\frac{2}{r_j}\right)(g_{\alpha j+1}^{(i+1)} - g_{\alpha j-1}^{(i+1)})/(2\delta r) - 2g_{\alpha j}^{(i+1)}/r_j^2\Bigg] - \\ z_\alpha\left[v_{1j}^{(i)} + \frac{D_\alpha z_\alpha}{2\delta r}(g_{\alpha j+1}^{(i+1)} - g_{\alpha j-1}^{(i+1)}) + D_\alpha z_\alpha b\right]\left(\frac{\partial y_0}{\partial r}\right)_j \end{aligned} \tag{36}$$

In principal, the $\nabla\cdot\mathbf{v}^{(i)}$ term can be neglected since the solution is incompressible. However, since the $\mathbf{v}^{(i)}$'s are

interpolated from numerical approximations of the true velocity field, it is included in some calculations. It can be written

$$(\nabla\cdot\mathbf{v}^{(i)})_j = (r_{j+1}{}^2 v_{1,j+1}^{(i)} - r_{j-1}{}^2 v_{1,j-1}^{(i)})/(2r_j{}^2\,\delta r) + 2v_{2j}^{(i)}/r_j \quad (37)$$

The reduced polyion potential, y_0, for a sphere is solved numerically following the algorithm of Loeb et al.[14] Following the same procedure, eq 30 becomes

$$\epsilon_{j+}(1+\delta r/2r_j)(f_{j+1}^{(i+1)} - f_j^{(i+1)})/\delta r^2 - \epsilon_{j-}(1-\delta r/2r_j)(f_j^{(i+1)} - f_{j-1}^{(i+1)})/\delta r^2 - 2f_j^{(i+1)}\epsilon_j/r_j{}^2 = \frac{4\pi q^2}{k_B T}\sum_\alpha z_\alpha{}^2 n_{\alpha 0}[f_j^{(i+1)} + p_{\alpha,j}^{(i+1)}] \quad (38)$$

where $p_{\alpha,j}^{(i+1)} = g_{\alpha,j}^{(i+1)} - g_{\alpha,j}^{(i)}$ and ϵ_{j+} and ϵ_{j-} are the dielectric constants at $r_j \pm \delta r/2$. It is straightforward to solve eq 36 and eq 38 by finite differences. Omit the $i+1$ superscript and α subscript. One starts with an initial guess of the g_j's and f_j's and then proceeds to obtain better estimates. Solving eq 36 for change in g_j using previous estimates for other quantities yields

$$\delta g_j = \Big[(\nabla\cdot\mathbf{v}^{(i)})_j/z + D(1+\delta r^2/4r_j^2)(g_{j+1} - 2g_j + g_{j-1})/\delta r^2 + D(g_{j+1} - g_{j-1})/r_j\,\delta r - (v_{1,j}^{(i)} + Dz(g_{j+1} - g_{j-1})/2\delta r + Dzb)\left(\frac{\partial y_0}{\partial r}\right)_j - 2Dg_j/r_j{}^2\Big]/(2D/\delta r^2 + 5D/2r_j{}^2)$$

$$g_{j,new} = g_{j,old} + \Omega\delta g_j \quad (39)$$

where Ω is a relaxation parameter which has been set to 1.8 in this work. A single iteration consists of the application of eqs 38 and 39 to all g_j's. This is repeated until

$$d_g = \sum_j \delta g_j{}^2 / \sum_j g_{j,old}{}^2 \quad (40)$$

converges to some tolerance level. We need g from $r = a$ to some maximum value, r_{max}. Far from the sphere, we must have $g = 0$. The variable r_{max} must be chosen large enough so that g near the sphere surface is independent of r_{max}. In the present work, we have chosen a constant radial spacing, δr. Let $r_j = (j-1)\delta r$ but choose δr such that $a = (i^* - 1)\delta r$ where i^* corresponds to the "lattice point" on the sphere surface. From the boundary condition following eq 21, we must have $g_{i^*} = g_{i^*+1} + b\delta r$. Thus, eqs 38 and 39 are solved iteratively from $j = i^* + 1$ to $j_{max} - 1$ where $j_{max} = r_{max}/\delta r$.

The corresponding finite difference equation for eq 38 is

$$\delta f_j = \frac{c_1 f_{j+1} + c_2 f_{j-1} - c_4}{c_1 + c_2 + c_3 + c_5} - f_j \quad (41)$$

$$f_{j,new} = f_{j,old} + \Omega\delta f_j \quad (42)$$

where

$$c_1 = \epsilon_{j+}(1 + \delta r/2r_j)/\delta r^2 \quad (43)$$

$$c_2 = \epsilon_{j-}(1 - \delta r/2r_j)/\delta r^2 \quad (44)$$

$$c_3 = 2\epsilon_j/r_j{}^2 \quad (45)$$

$$c_4 = 4\pi q^2\lambda\sum_\alpha z_\alpha{}^2 n_{\alpha 0} g_{\alpha,j}^{(i+1)}/k_B T \quad (46)$$

$$c_5 = 4\pi q^2\lambda\sum_\alpha z_\alpha{}^2 n_{\alpha 0}/k_B T \quad (47)$$

The correction potential, f, must be evaluated inside as well as outside the spherical polyion which requires some attention be paid to the dielectric discontinuity and screening parameter. We shall assume $\lambda = 0$ for $r < a$ and $\lambda = 1$ for $r > a$ which is equivalent to placing the solvent-accessible surface at $r = a$. The dielectric function is taken to be

$$\epsilon(r) = \begin{cases} \epsilon_1 & r < a - \Delta \\ \epsilon_1 + (r - a + \Delta)(\epsilon_2 - \epsilon_1)/\Delta & \text{for } a - \Delta < r < a \\ \epsilon_2 & r > a \end{cases} \quad (48)$$

where Δ is left as an adjustable parameter. It is interesting to note that O'Brien and White[12] have shown that the electrophoretic mobility is independent of ϵ_1 for a spherical polyion containing a centrosymmetric charge distribution.

The boundary conditions on f_j are $f_1 = f_{j,max} = 0$. Equation 41 is applied repeatedly until the f_j's converge to some tolerance level, d_f

$$d_f = \sum_j \delta f_j{}^2 / \sum_j F_j{}^2 \quad (49)$$

where F_j is a total correction potential defined by

$$y(r,\theta) - y_0(r) = F(r)\cos\theta \quad (50)$$

The finite difference (fd) calculations start on a coarse grid with a typical starting grid spacing of 0.2 nm. Once convergence is achieved the fd results are used as starting values for a new fd calculation for both g_α and f on a finer grid with a grid spacing of half that used before. This is repeated a number of times until some minimum grid separation, δr_{min}, is achieved. A typical value of δr_{min} in this work is 0.001 563 nm.

Once $\{g_{\alpha,j}^{(i+1)}\}$ and $\{f_j^{(i+1)}\}$ have been solved by finite difference, it is possible to calculate the external forces, $\mathbf{s}(\mathbf{x})$, on the fluid according to eq 24. The change in the external forces between successive iterations can be written (assuming $\delta\rho$ and δy are small compared to ρ_0 and y_0)

$$\mathbf{s}^{(i+1)} - \mathbf{s}^{(i)} = -k_B T q^{-1}[\rho_0\nabla(y^{(i+1)} - y^{(i)}) + (\rho^{(i+1)} - \rho^{(i)})\nabla y_0] \quad (51)$$

Let r be the distance of a fluid point, $\mathbf{x}$, from the origin of a sphere and θ the angle between $\mathbf{x}$ and the flow direction (along the 1 axis). Then the force components can be written as

$$s_1^{(i+1)} - s_1^{(i)} = -k_B T\sum_\alpha n_{\alpha 0} z_\alpha[\cos^2\theta f'^{(i+1)} + \sin^2\theta f^{(i+1)}/r - z_\alpha\cos^2\theta y_0'(f^{(i+1)} + p_\alpha{}^{(i+1)})] \quad (52)$$

$$s_2^{(i+1)} - s_2^{(i)} = -k_B T\sum_\alpha n_{\alpha 0} z_\alpha\cos\theta\sin\theta[f'^{(i+1)} - f^{(i+1)}/r - z_\alpha y_0'(f^{(i+1)} + p_\alpha^{(i+1)})] \quad (53)$$

where primes denote a radial derivative ($\partial/\partial r$) and the 2

subscript the vector component perpendicular to 1 but in the plane formed by $\mathbf{x}$ and the 1 axis. These force components are then used to calculate the updated stress forces on the polyion, $\mathbf{f}^{(i+1)}$ (eq A28), and the new velocity field, $\mathbf{v}^{(i+1)}$ (eqs A12 and A22). As discussed in Appendix A, the space around the polyion is divided into M spherical shells which extend far enough into the solution to insure that the contribution of external forces from more distant regions of the solution make negligible contributions to the stress forces and velocity field. Typically, $M = 100$ and with $a = 2$ nm, the shells extend out to a distance of about 4.5 nm so the shell thickness is about 0.025 nm. Since this is much larger than the lattice spacing used in the fd calculations, δr_{min}, it is straightforward to interpolate f, f', and p_α to calculate the correction forces defined by eqs 52 and 53. Once the f_i's are computed, eq A30 is used to calculate the hydrodynamic force on the polyion, $\mathbf{z}_h$.

The remaining quantity that needs to be determined is the electrostatic force defined by eqs 5 and 6; provided δy is small compared to y_0, it is possible to solve for a spherical particle of radius a containing a centrosymmetric charge distribution

$$\mathbf{z}_e^{(i+1)} = \frac{\epsilon_2(k_BT)^2 y_0'(a)}{4\pi q^2}\int_{s_p} \nabla(y^{(i+1)} - y_0)\, dA \qquad (54)$$

If the net charge of the polyion is Q (in units of the protonic charge), then

$$y_0'(a) = -q^2Q/\epsilon_2 k_BTa^2 \qquad (55)$$

regardless of the ionic atmosphere. It should be emphasized that the charge Q can be placed at the center of the sphere, uniformly distributed on the surface, or distributed in any manner in the sphere interior as long as it is centrosymmetric and adds up to a net charge of Q. It is straightforward to show

$$\nabla(y^{(i+1)} - y_0) = \mathbf{i}\cos\phi\, h_1(r,\theta) + \mathbf{j}\sin\phi\, h_1(r,\theta) + \mathbf{k}h_2(r,\theta) \qquad (56)$$

where

$$h_1(r,\theta) = \cos\theta\sin\theta[F^{v(i+1)}(r) - F^{(i+1)}(r)/r]$$

$$h_2(r,\theta) = \cos^2\theta F^{v(i+1)}(r) - \sin^2\theta F^{(i+1)}(r)/r \qquad (57)$$

Combining eqs 54 and 57 yields finally

$$z_{e1}^{(i+1)} = -k_BTQ(F^{v(i+1)}(a) + 2F^{(i+1)}(a)/a)/3 \qquad (58)$$

and $z_{e2}^{(i+1)} = 0$.

IV. Results

From the discussion of the algorithm in the previous section, it is clear that a number of parameters must be investigated to see how they effect the electrostatic and hydrodynamic forces acting on the polyion. On the basis of the work of Wiersema et al.[10,11] and others,[12] there are many test cases available with which we can compare our numerical electrophoretic mobilities. We shall choose a polyion radius of $a = 2$ nm immersed in a monovalent salt solution of dielectric constant $\epsilon_2 = 78$ with an ambient salt concentration of 0.576 M. The temperature and solution viscosity are taken to be 25 °C and 0.0089 P, respectively. This gives $\kappa a = 5$ where κ is the Debye–Hückel screening parameter. Since the mobilities of the co-ions and counterions enter the problem through the ion-transport equation (eq 14), we shall assume an effective hydrodynamic radius, $a_\pm = 0.132$ nm for both co-ions and counterions. This gives $m_\alpha = 0.184$ ($\alpha = +1$ or -1) where

$$m_\alpha = \epsilon_2 k_BTf_\alpha/6\pi\eta q^2 \qquad (59)$$

and $f_\alpha = k_BT/D_\alpha = 6\pi\eta a_\alpha$ is the friction coefficient of ion α. This value of m_α was used extensively by Wiersema et al. The limiting equivalent conductance of α, $\lambda_\alpha°$, is related to f_α by

$$f_\alpha = N_{Av}q^2z_\alpha/\lambda_\alpha° \qquad (60)$$

where N_{Av} is Avogadro's number. This choice of a_α corresponds to a $\lambda_\alpha°$ of 70 Ω^{-1} cm^2 eq^{-1} and is fairly typical of monovalent ions ($\lambda°$ = 50.10 and 76.35 for Na^+ and Cl^-, respectively).

In the results presented in the next few paragraphs, a reduced surface potential of $y_0 = 3$ is assumed which corresponds to a net polyion charge of $+66.33q$. This value is large enough to insure that ion relaxation effects are significant. In a combined finite difference/iterative algorithm as is used here, two important questions are, how sensitive are the results to the grid spacing used in finite differences and how quickly do they converge from one iterative cycle to the next? Shown in Table 1 are $g_-(2.0)$ and $f(2.0)$ (evaluated at the polyion surface, $r = 2$ nm) as a function of δr_{min} and cycle for a case 2 example ($u_0 = 0$, $e_0 = 1$ kV/cm). Parameters other than those given above are $\epsilon_1 = 2$, $\Delta = 0.0125$ nm, $r_{max} = 50$ nm, $N = 10$ (number of angular divisions), $M = 100$ (number of radial shells), $d_g = 10^{-11}$, and $d_f = 10^{-18}$. To four significant figures, $g_-(2.0)$ is fully converged for a grid spacing less than or equal to 0.006 25 nm. The dependence of $g_+(2.0)$ on δr_{min} is substantially weaker (results not shown). A smaller δr_{min} of 0.001 563 nm is required to obtain $f(2.0)$ to the same degree of accuracy. This is due, in part, to the dielectric discontinuity at the polyion surface. Increasing ϵ, from 2 to 78 (no dielectric discontinuity), a δr_{min} of about 0.0031 nm is required to obtain $f(2.0)$'s converged to four significant figures. With regard to the number of cycles required, Table 1 shows that four are required in this case. However, the number increases as y_0 increases. For $y_0 = 5$, at least six iteration cycles are required. Table 2 shows the corresponding dependence of the total reduced correction potential at the ion surface, $F(2.0)$. Its behavior reflects $f(2.0)$ closely. When d_f (the cutoff parameter used in the fd determination of f) is reduced from 10^{-18} to 10^{-20} in order to obtain more highly converged f's, the resulting F's are identical to those given in Table 2. The effect of grid spacing on the forces $z_{h1}^{(2)}$, $z_{e1}^{(2)}$, and $z_{t1}^{(2)}$ is shown in Figure 1. Model parameters are the same as in the previous paragraph. Differences are plotted in units of 10^{-11} dyn. These represent the end result of seven cycles of relaxation, and the absolute forces for $\delta r_{min} = 0.000\ 781$ nm are $z_{h1}^{(2)}$, $z_{e1}^{(2)}$, $z_{t1}^{(2)} = 0.5082 \times 10^{-7}$, -0.6317×10^{-7}, -0.1235×10^{-7} dyn, respectively. The relative errors between $\delta r_{min} = 0.00625$ and 0.00781 nm for $z_{h1}^{(2)}$, $z_{e1}^{(2)}$, and $z_{t1}^{(2)}$ amount to be 1.2, 1.3, and 1.6%. These forces are more sensitive to grid spacing than g_α, f, and F, and the reason for this is that they depend on the gradient of F which is a more sensitive function of grid resolution.

Table 3 shows how z_{h1}, z_{e1}, and z_{t1} depend on the iteration cycle for the same example discussed in the previous paragraph with $\delta r_{min} = 0.001\ 563$ nm. Case 1 results (translating polyion in the absence of an external field) are presented along with case 2. In case 1, u_0 has been chosen to give a total force equal but opposite in sign to that of case 2 after several cycles. In the case of cycle 0, external forces are calculated in the absence of any relaxation of the ion atmosphere. Cycle 1 forces account for ion relaxation, but the velocity field used to calculate this ion relaxation is based on the unrelaxed ion distri-

Table 1. Dependence of $g_-(2.0)$ and $f(2.0)$ on Grid Resolution and Cycle for $y_0 = 3$, $\kappa a = 5$, Case 2

δr_{min} (nm)	cycle 1	2	3	4	7
			$g_-(2.0) \times 10^2$		
0.025	0.1705	0.1450	0.1465	0.1464	0.1464
0.012 5	0.1781	0.1538	0.1553	0.1552	0.1552
0.006 25	0.1783	0.1541	0.1555	0.1554	0.1554
0.003 125	0.1783	0.1541	0.1555	0.1554	0.1554
0.001 563	0.1783	0.1541	0.1555	0.1554	0.1554
0.000 781 3	0.1783	0.1541	0.1555	0.1554	0.1554
			$f(2.0)$		
0.025	-0.4887×10^{-2}	0.2419×10^{-3}	-0.1449×10^{-4}	-0.8644×10^{-6}	-0.2240×10^{-9}
0.012 5	-0.4921×10^{-2}	0.2301×10^{-3}	-0.1376×10^{-4}	-0.8644×10^{-6}	-0.2240×10^{-9}
0.006 25	-0.4903×10^{-2}	0.2297×10^{-3}	-0.1376×10^{-4}	-0.8644×10^{-6}	-0.2240×10^{-9}
0.003 125	-0.4894×10^{-2}	0.2297×10^{-3}	-0.1376×10^{-4}	-0.8644×10^{-6}	-0.2240×10^{-9}
0.001 563	-0.4890×10^{-2}	0.2297×10^{-3}	-0.1376×10^{-4}	-0.8644×10^{-6}	-0.2240×10^{-9}
0.000 781 3	-0.4890×10^{-2}	0.2297×10^{-3}	-0.1376×10^{-4}	-0.8644×10^{-6}	-0.2240×10^{-9}

Table 2. Dependence of $F(2.0)$ on Grid Resolution and Cycle for $y_0 = 3$, $\kappa a = 5$, Case 2, $F(2.0) \times 10^2$

δr_{min}	cycle 0[a]	1	2	3	4	7
0.025	1.152	0.6633	0.6875	0.6860	0.6861	0.6861
0.012 5	1.152	0.6599	0.6829	0.6815	0.6816	0.6816
0.006 25	1.152	0.6617	0.6847	0.6833	0.6834	0.6834
0.003 125	1.152	0.6626	0.6856	0.6842	0.6843	0.6843
0.001 563	1.152	0.6630	0.6860	0.6846	0.6847	0.6847
0.000 781 3	1.152	0.6630	0.6860	0.6846	0.6847	0.6847

[a] From eqs 28 and 50.

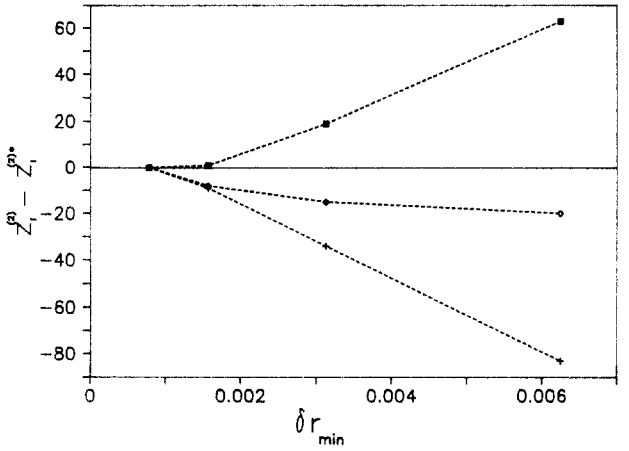

Figure 1. Effect of grid resolution on net polyion forces for case 2: $y_0 = 3$, $\kappa a = 5$, $\epsilon_1 = 2$. The grid resolution, δr_{min}, is in nanometers and $a = 2$ nm. $z_1^{(2)*}$ represents the net force for the highest resolution run ($\delta r_{min} = 0.000\ 778\ 1$ nm) and differences in forces are in units of 10^{-11} dyn. Squares (top curve), crosses (bottom curve), and diamonds (middle curve) correspond to differences in $z_{h1}^{(2)}$, $z_{e1}^{(2)}$, and $z_{t1}^{(2)}$, respectively.

Table 3. Dependence of z_{h1}, z_{e1}, z_{t1} on the Iteration Cycle for $y_0 = 3$, $\kappa a = 5$[a]

cycle	$z_{h1}^{(1)}$ [b]	$z_{h1}^{(2)}$ [c]	$z_{e1}^{(1)}$	$z_{e1}^{(2)}$	$z_{t1}^{(1)}$	$z_{t1}^{(2)}$
0	0.1224	0.9056	0.0000	−1.062	0.1224	−0.1562
1	0.1066	0.4905	0.0178	−0.6127	0.1244	−0.1221
2	0.1077	0.5094	0.0166	−0.6338	0.1243	−0.1245
3	0.1076	0.5083	0.0167	−0.6326	0.1243	−0.1243
4	0.1076	0.5083	0.0167	−0.6326	0.1243	−0.1243
7	0.1076	0.5083	0.0167	−0.6326	0.1243	−0.1243

[a] Forces are in 10^{-7} dyn. [b] Case 1 forces with $e_0 = 0$, $u_0 = 0.365$ cm/s. [c] Case 2 forces with $e_0 = 1$ kV/cm, $u_0 = 0$.

bution. Before cycle 2 is started, a new velocity field is calculated using the relaxed ion distribution calculated in cycle 1. This process is then repeated several times. It is clear from this table that ion relaxation has a significant effect on the hydrodynamic and electric forces acting on the polyion and that about four cycles are required to obtain convergence. It is also clear that case 1 results are less sensitive to ion relaxation than case 2. This is true for other input parameters as well so the following discussion will be confined primarily to case 2 results.

Table 4. Reduced Mobilities for Different y_0

y_0	u_{red}	error (%)[a]	y_0	u_{red}	error (%)[a]
1[b]	1.121	−1.1	5[c]	3.050	−3.8
3[b]	2.724	−0.7	5[d]	3.090	−2.5
5[b]	2.850	−10.1	5[e]	3.099	−2.2

[a] Percent deviation from the Wiersema[8,9] value. [b] $N = 15$, $M = 100$, $\epsilon_{in} = 2$. [c] $N = 15$, $M = 200$, $\epsilon_{in} = 2$. [d] $N = 15$, $M = 300$, $\epsilon_{in} = 2$. [e] $N = 15$, $M = 100$, $\epsilon_{in} = 78$.

The number of angular divisions, N, into which the sphere is divided will not directly influence the finite difference results but will affect the forces on the polyion and also the velocity field around the polyion. Although g_α depends on the velocity field and will therefore depend indirectly on N, the effect on g_α is observed to be very small. For the example considered previously ($\delta r_{min} = 0.001\ 563$ nm) $z_{t1}^{(2)} = -0.1321 \times 10^{-7}$, -0.1243×10^{-7}, and -0.1232×10^{-7} dyn for $N = 5$, 10, and 15, respectively. Thus, an N value in the range 10–15 is expected to give accurate forces. For $y_0 = 3$, the net forces on the polyion are not sensitive to the number of radial shells, M, at which external forces are calculated (see the appendix) provided this parameter is set to 100 or higher. However, for larger y_0, a larger M should be used as discussed later in connection with $y_0 = 5$ cases.

The cutoff parameters d_g and d_f as well as r_{max} are important with regard to the finite difference calculations. How they influence z_{t1} shall be discussed briefly. For $d_g = 10^{-9}$, 10^{-10}, 10^{-11}, and 10^{-12}, $z_{t1}^{(2)} = -0.1254$, -0.1247, -0.1243, and -0.1240×10^{-7} dyn, respectively. This is for the same $y_0 = 3$, case 2 example considered previously with $\delta r_{min} = 0.001\ 563$ nm, $N = 10$, and $M = 100$. For $d_f = 10^{-15}, 10^{-16}, 10^{-17}, 10^{-18}$, and 10^{-20}, $z_{t1}^{(2)} = -0.1182, -0.1220, -0.1232, -0.1243$, and -0.1248×10^{-7} dyn, respectively. Reducing r_{max} from 50 to 12.5 nm changes $z_{t1}^{(2)}$, from -0.1243 to -0.1239×10^{-7}, holding all other input parameters constant. In the remainder of this work, we shall set d_g, d_f, and r_{max} to 10^{-11}, 10^{-18}, and 50 nm, respectively.

As discussed previously, determination of the electrophoretic mobility requires z_{t1} for a translating polyion in the absence of an external field ($z_{t1}^{(1)}$) and a stationary polyion in the presence of an external field ($z_{t1}^{(2)}$). The mobility is then given by eq 9. Shown in Table 4 are reduced mobilities (eq 10) for the cases $y_0 = 1$, 3, and 5. They can be compared with the results of Wiersema[10,11] which predict $\mu_{red} = 1.134$, 2.742, and 3.169 for $y_0 = 1$, 3, and 5, respectively. In each case, $\kappa a = 5$ and $m_\alpha = 0.184$. For $y_0 = 1$ and 3, the finite difference approach is in excellent agreement with earlier predictions. For $y_0 = 5$,

Table 5. Summary of Forces[a] on Polyion with and without Relaxation

y_0	ϵ_1	case	ion relaxation	z_{h1}	z_{e1}	z_{t1}	u^b
1	2	1	no	0.05107	0	0.05107	0.152
1	2	2	no	0.2247	−0.2757	−0.05107	0
1	2	1	yes	0.04942	0.00085	0.05010	0.149
1	2	2	yes	0.2128	−0.2629	−0.05010	0
3	2	1	no	0.1553	0	0.1553	0.463
3	2	2	no	0.9066	−1.062	−0.1553	0
3	2	1	yes	0.1067	0.01654	0.1232	0.361
3	2	2	yes	0.5093	−0.6325	−0.1232	0
3	78	1	no	0.1309	0	0.1309	0.390
3	78	2	no	0.9310	−1.062	−0.1309	0
3	78	1	yes	0.10084	0.02274	0.1236	0.363
3	78	2	yes	0.7451	−0.8687	−0.1236	0
5	2	1	no	0.2556	0	0.2556	0.762
5	2	2	no	2.581	−2.837	−0.2556	0
5	2	1	yes	0.08901	0.05309	0.1421	0.410
5	2	2	yes	0.5774	−0.7195	−0.1421	0
5	78	1	no	0.2229	0	0.2229	0.664
5	78	2	no	2.614	−2.837	−0.2229	0
5	78	1	yes	0.06762	0.07556	0.1432	0.411
5	78	2	yes	0.8931	−1.036	−0.1432	0

[a] Forces are in 10^{-7} dyn. [b] Velocities are in cm/s.

the results are less satisfactory. Nonetheless, by simply increasing M (calculating the external forces on the solution using a finer grid) much of the discrepancy can be removed. Alternatively, using a dielectric constant of 78 to remove the dielectric discontinuity at the polyion surface yields a mobility in fairly good agreement with the Wiersema value even with M = 100. On the basis of the results presented in Table 4, we conclude that the DIE/finite difference approach is capable of handling ion relaxation to sufficient accuracy to yield electrophoretic mobilities correct to within a few percent of their actual values.

Table 5 summarizes the main results of this paper. Each block of four entries treats a single y_0, ϵ, combination. Within each block of four, the first pair of entries deals with polyions in the absence of ionic relaxation and the latter with relaxation. Within a pair, the first line represents a case 1 polyion translating with sufficient velocity to insure the total force just cancels the case 2 polyion, which is stationary with an external field of 1 kV/cm acting on it. Adding together the forces, electric fields, and velocities of a pair will thus give us a translating polyion with no net force acting on it. For y_0 = 1, ionic relaxation has little effect on the net hydrodynamic ($0.2758/0.2622 \times 10^{-7}$ dyn without/with relaxation), net electrostatic ($-0.2758/-0.2622 \times 10^{-7}$ dyn without/with relaxation), or steady-state ion velocity (0.152/0.149 cm s^{-1} without/with relaxation). However, relaxation is seen to reduce the net hydrodynamic (or electrostatic) force on the polyion and at the same time it reduces u. This behavior is seen at higher y_0 as well. Table 5 helps us understand why case 1 results are much less sensitive to factors such as grid spacing in finite differences. In case 2 (regardless of ion relaxation) z_{h1} and z_{e1} are of comparable magnitude but opposite in sign. The total force is thus the difference between two large numbers of comparable magnitude so small relative errors in z_{h1} and/or z_{e1} can lead to much larger relative errors in z_{t1}. This is not a problem in case 1.

In the presence of ion relaxation, the electrophoretic velocity is independent of ϵ_1 on the basis of Tables 4 and 5. This was also observed by Wiersema.[10,11] This appears to be a special case of a general truth that the electrophoretic mobility of a rigid polyion depends only on its size and shape, the properties of the associated electrolyte solution, and the charge within its hydrodynamic shear plane.[12] (Although this does not appear to be true for the no relaxation case, it is probably not meaningful to discuss the dependence of the electrophoretic velocity on the dielectric constant when ion relaxation is suppressed since this corresponds to the unphysical situation of allowing the solvent around the polyion to relax but not the ion atmosphere.) Even though the electrophoretic velocity is independent of ϵ_1 for the cases considered in this work, the hydrodynamic and electrostatic forces are not the same. For y_0 = 3 and an external field of 1 kV/cm, for example, the electrophoretic velocity is about 0.41 cm/s independent of ϵ_1, but the total hydrodynamic force will be 0.6160×10^{-7} dyn for ϵ_1 = 2 but 0.8459×10^{-7} dyn for ϵ_1 = 78. These forces are balanced by electrostatic forces of equal magnitude but opposite sign.

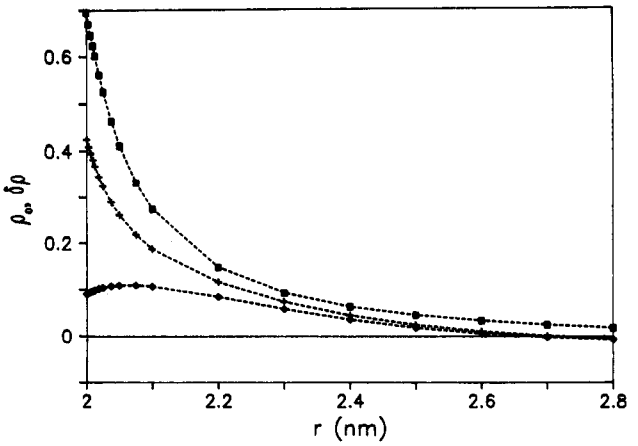

Figure 2. Net charge (ρ_0) and perturbed charged densities ($\delta\rho$) for y_0 = 3, κa = 5, along the flow direction (+x axis). The electric field and ion velocity are 1 kV/cm and 0.36 cm/s, respectively, directed along the −x axis. The polyion surface is at r = 2 nm. Units of ρ_0 (squares) are in 10^1 electron charge nm^{-3}, while $\delta\rho$ for ϵ_1 = 2 (crosses) and ϵ_1 = 78 (diamonds) are in 10^{-2} electron charge nm^{-3}, respectively.

Plotted in Figure 2 are the ion densities along the flow direction for y_0 = 3, e_0 = 1 kV/cm, and u = 0.36 cm/s. Perturbed ion densities (crosses for ϵ_1 = 2 and diamonds for ϵ_1 = 78) have been multiplied by 1000 relative to unperturbed ion densities (squares). Under the stated conditions, this perturbation is seen to be very small, less than 0.1%, despite the fact z_{h1} and z_{e1} change by 40%. The physical basis for this can be understood by reviewing the terms which contribute to the external forces on the solvent, **s**. Retaining terms linear in $\delta\rho$ and δy, eq 24 becomes

$$\mathbf{s} = -k_B T q^{-1}[\rho_0 \nabla y_0 + \rho_0 \nabla \delta y + \delta\rho \nabla y_0] \qquad (61)$$

The first term on the right-hand side represents the equilibrium ion distribution, ρ_0, interacting with the electric field of the polyion itself, and this makes no *net* contribution to z_{h1} or z_{e1}. The second term represents the interaction of ρ_0 with the perturbing electric field ($k_B T q^{-1} \nabla \delta y$), and this is the only contributing element in the absence of ion relaxation. The final term represents the interaction of the perturbed ion distribution with the electric field of the polyion itself. Although $\delta\rho$ is small relative to ρ_0, it is also true that ∇y_0 is large relative to $\nabla \delta y$ which means that the second and third terms may be comparable in magnitude. Also, reducing e_0 will not alter the situation since δy and $\delta\rho$ scale linearly with e_0 at low fields.

The last two figures show how ion relaxation affects the velocity field around the polyion relative to the unrelaxed case. In order to make the comparison straightforward, the electric field (directed along −x) has been adjusted to

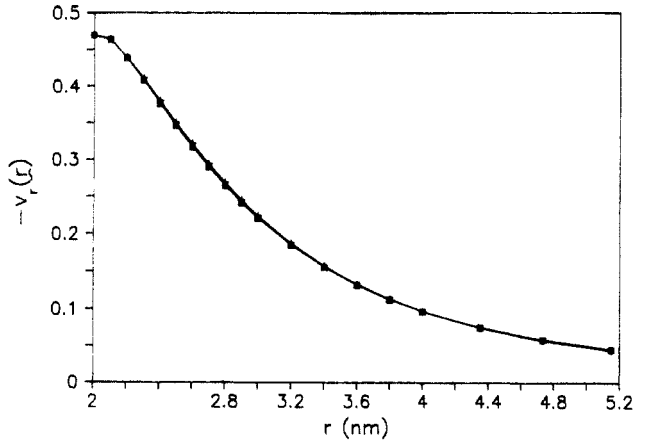

Figure 3. Effect of ion relaxation on $-v_r$ along the flow ($+x$) direction for $y_0 = 3$ and $\kappa a = 5$. Nonrelaxation (squares) and relaxation (crosses) cases involve 2-nm radius polyions placed in an electric field (along $-x$) strong enough to insure a steady-state velocity of 0.47 cm/s (along $-x$).

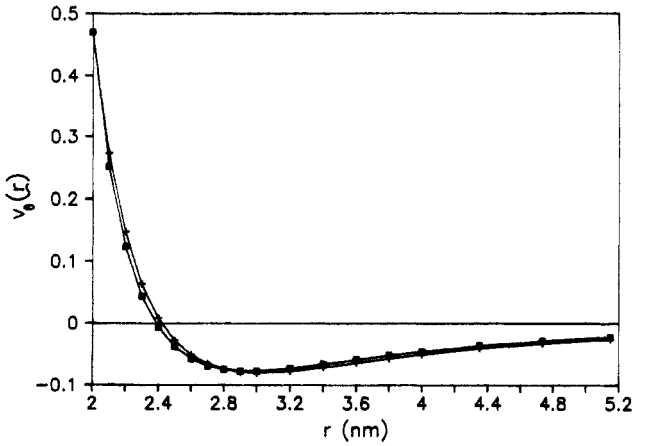

Figure 4. Effect of ion relaxation on $+v_\theta$ along an axis perpendicular to the flow ($+x$) direction for $y_0 = 3$ and $\kappa a = 5$. See the caption to Figure 3 for details. The unit vector, $\hat{e}_\theta$, is directed along $-x$ in this case.

insure the velocity of the ion (also directed along $-x$) is 0.47 cm/s. Plotted in Figure 3 is $-v_r$ versus r along the $+x$ axis for the case $y_0 = 3$, $\kappa a = 5$, $a = 2$ nm, and $\epsilon_1 = 2$. Squares and crosses correspond to velocity fields without and with relaxation. Figure 4 is similar but shows $+v_\theta$ along an axis perpendicular to the flow ($+x$) direction. Although there are differences between the velocity fields with and without relaxation, they are seen to be small.

V. Summary

Previously, a DIE algorithm was developed and applied to the electrophoresis of polyions modeled as a rigid body in the absence of ionic relaxation.[1] In the present work, this was extended to include the effects of ion relaxation by combining the DIE algorithm to solve the Navier–Stokes equation with the technique of finite differences to solve the Poisson and ion-transport equations. This combined DIE/finite difference algorithm has been applied to the special case of a spherical polyion containing a centrosymmetric charge distribution. Electrophoretic mobilities are in excellent agreement with those obtained by other methods which shows that the algorithm is definitely working.

In applying the algorithm to the spherical case, we have been able to reduce the finite difference equations from three to one dimensions. Under these conditions it is possible to use grids of very high resolution extending far out into solution. Since perturbations in the charge density less than 0.1% from the equilibrium distribution can alter the net force on the polyion by 40%, it is clear that perturbed potentials and charge densities of high accuracy are required. Application of this approach to polyions of *arbitrary* shape and charge distribution appears to be straightforward in principal but formidable in practice because of the required accuracy involved. Finite difference methods applied to solving the Poisson–Boltzmann equation in three dimensions on a Cartesian lattice typically have a grid resolution of 0.1–0.2 nm and yield electrostatic potentials accurate to several percent.[15–20] Early in the course of our work on the electrophoresis of spheres, we attempted to use three-dimensional Cartesian lattices to solve the Poisson and ion-transport equations. Unfortunately, the results were too inaccurate to yield meaningful electrophoretic mobilities. Finite element[26,27] as well as multigrid refinements[28,29] of finite difference methods may be more effective in dealing with this problem. In any case, more efficient methods are needed to solve the ion-transport and Poisson equations for a general polyion (eqs 29 and 30) since these were unquestionably the computational "bottleneck" in this work. It may also be feasible to improve the solution of Stokes equations. The integral equation algorithm employed here and elsewhere[1,5,6] involves the solution of Fredholm equations of the first kind which are known to be ill-posed. In other words, numerical solutions tend to be unstable. Kim and co-workers[30,31] have developed an algorithm based on solution of Fredholm equations of the second kind which avoids the numerical instabilities of the "first kind" formulation. To the best of our knowledge, however, no study comparing the two approaches explicitly has been published. There are, however, a number of special cases where the algorithm presented in this work may find use. The first is in the case of a sphere containing an electric dipole lying along the flow direction. This straightforward problem would shed light on how the distribution of charge affects the mobility. A very important application is the electrophoresis of rodlike molecules since this is a reasonable model for DNA.[32–35] A charged-rod model in cylindrical coordinates may be feasible.

Alternatively, ion relaxation may be unimportant in many cases which greatly simplifies the problem. Most proteins, for example, contain low net charges so the average surface potentials are low under physiological conditions. At a monovalent salt concentration of 0.1 M, a 2-nm radius sphere containing a central charge of $\pm 18.85q$ has a reduced surface potential of ± 2.0. Ionic relaxation reduces the electrophoretic mobility of this "protein" by only 10% and the effect decreases as the absolute value of the net charge decreases. Since this model "protein" is more highly charged than most real ones, ignoring ion relaxation may be a good approximation. The problem then resorts to solving the DIE portion of the problem though finite differences will still be required to determine the equilibrium charge density and the electrostatic potential around the (equilibrium) polyion in the presence of an external field.

In any case, it is hoped that the present work will stimulate renewed interest in the electrophoresis of polyions. We anticipate numerical algorithms of the kind described here will play an important role in this development.

Acknowledgment. We acknowledge Grant GM46516-01 from the National Institutes of Health for partial support of this work.

Appendix

Consider an arbitrary rigid body moving through an unbounded incompressible fluid with velocity $-\mathbf{u}(\mathbf{x})$. Far

from the body, the fluid velocity, $\mathbf{v}(\mathbf{x})$, is taken to vanish. At low Reynolds number, the solution of the Navier–Stokes equation yields

$$\mathbf{v}(\mathbf{x}) = \mathbf{v}^a(\mathbf{x}) + \mathbf{v}^b(\mathbf{x}) + \mathbf{v}^c(\mathbf{x}) \tag{A1}$$

where

$$\mathbf{v}^a(x) = -\int\int\int_\Omega \mathbf{U}(\mathbf{x},\mathbf{y})\cdot\mathbf{s}'(\mathbf{y})\, d^3y \tag{A2}$$

$$\mathbf{v}^b(\mathbf{x}) = -\int\int \mathbf{U}(\mathbf{x},\mathbf{y})\cdot\mathbf{f}'(\mathbf{y})\, dS_y \tag{A3}$$

$$\mathbf{v}^c(x) = -\frac{3}{4\pi}\int\int_{S_p} r^{-3}\, \mathbf{r}\cdot(\mathbf{v}(\mathbf{y})\cdot\mathbf{R}(\mathbf{x},\mathbf{y})\cdot\mathbf{n}(\mathbf{y}))\, dS_y \tag{A4}$$

and $\mathbf{r} = \mathbf{x} - \mathbf{y}$, $r = |\mathbf{r}|$,

$$(\mathbf{R}(\mathbf{x},\mathbf{y}))_{ij} = r_i r_j / r^2 \tag{A5}$$

$$\mathbf{U}(\mathbf{x},\mathbf{y}) = \frac{1}{8\pi\eta\mathbf{r}}[\mathbf{I} + \mathbf{R}(\mathbf{x},\mathbf{y})] \tag{A6}$$

η is the solvent viscosity, Ω denotes the volume of fluid external to the rigid body, and S_p denotes the surface of the rigid body. In eq A2, $\mathbf{s}'(\mathbf{x})$ is the force per unit volume acting on the fluid at $\mathbf{x}$ due to external forces. In eq A3, $\mathbf{f}'(\mathbf{y})$ is the stress force per unit area on the fluid due to the rigid body at position $\mathbf{y}$ on its surface. These forces are the same as those appearing in eqs 1 and 2 in the main text. The primes have been introduced to distinguish the normal three-dimensional forces (denoted by the primes) from the corresponding two-dimensional quantities introduced later in this appendix. In eq A4, $\mathbf{n}(\mathbf{y})$ denotes the *inward* unit normal to the rigid-body surface at $\mathbf{y}$.

If stick boundary conditions are assumed, then $\mathbf{v}(\mathbf{x}) = -\mathbf{u}(\mathbf{x})$ at the surface of the body. For a case of a rigid particle undergoing purely translational motion, it can be shown that

$$\mathbf{v}^c(\mathbf{x}) = \begin{cases} 0 & \mathbf{x} \in \Omega \\ +\mathbf{u}/2 & \mathbf{x} \in S_p \\ +\mathbf{u} & \mathbf{x} \in \Omega' \end{cases} \tag{A7}$$

where Ω' denotes the interior volume of the polyion. Equation A7 can be proven by applying Green's theorem to the Navier–Stokes equation as described on pp 51–54 of Ladyzhenskaya.[4] However, the proof given in ref 4 is incorrect. The error has to do with the fact that a surface integral at an infinite distance from a rigid body does not in fact vanish when the fluid velocity field is constant (and nonzero). When this is taken into account, Ladyzhenskaya's arguments yield eq A7. Equation A7 can also be verified by direct numerical integration. Thus eq A1 becomes

$$\mathbf{v}(\mathbf{x}) = \mathbf{v}^a(\mathbf{x}) + \mathbf{v}^b(\mathbf{x}) \qquad \mathbf{x} \in \Omega \tag{A8}$$

and in the limit $\mathbf{x}$ approaches the rigid-body surface from the external or fluid side

$$-\mathbf{u} = \mathbf{v}^a(\mathbf{x}) + \mathbf{v}^b(\mathbf{x}) \qquad \mathbf{x} \in S_p \tag{A9}$$

Unlike $\mathbf{v}^c$, $\mathbf{v}^a$ and $\mathbf{v}^b$ are continuous at the surface of the particle.

Equations A2 and A3 can be simplified further for axially symmetric structures translating along the axis of symmetry. Consider a sphere of radius a translating along the x direction. The stress, external force, and fluid velocity forces can be written as

$$\begin{aligned} f'_x &= f_1(\theta) \\ f'_y &= f_2(\theta)\cos\phi \\ f'_z &= f_2(\theta)\sin\phi \end{aligned} \tag{A10}$$

$$\begin{aligned} s'_x &= s_1(r,\theta) \\ s'_y &= s_2(r,\theta)\cos\phi \\ s'_z &= s_2(r,\theta)\sin\phi \end{aligned} \tag{A11}$$

$$\begin{aligned} v_x &= w_1(r,\theta) \\ v_y &= w_2(r,\theta)\cos\phi \\ v_z &= w_2(r,\theta)\sin\phi \end{aligned} \tag{A12}$$

where (r, θ, ϕ) denote the spherical coordinates of some point. The stress forces are evaluated at the surface of a sphere ($r = a$). It proves convenient to define 2×1 column vectors

$$\mathbf{w}(r,\theta) = \begin{pmatrix} w_1(r,\theta) \\ w_2(r,\theta) \end{pmatrix} \tag{A13}$$

with similar definitions for $\mathbf{f}(\theta)$ and $\mathbf{s}(r,\theta)$. Integrating eqs A2 and A3 over ϕ leads to

$$\mathbf{w}(r',\theta') = \mathbf{w}^a(r',\theta') + \mathbf{w}^b(r',\theta') \tag{A14}$$

where

$$\mathbf{w}^a(r',\theta') = \frac{1}{8\pi\eta}\int_a^\infty r^2\, dr \int_0^\pi \sin\theta\, d\theta\, \mathbf{G}(r,r',\theta,\theta')\cdot\mathbf{s}(r,\theta) \tag{A15}$$

$$\mathbf{w}^b(r',\theta') = \frac{1}{8\pi\eta}\int_0^\pi \sin\theta\, d\theta\, \mathbf{G}(a,r',\theta,\theta')\cdot\mathbf{f}(\theta) \tag{A16}$$

and

$$\mathbf{G} = \begin{pmatrix} G_{11} & G_{12} \\ G_{21} & G_{22} \end{pmatrix} \tag{A17}$$

$$G_{11}(r,r',\theta,\theta') = 2y^{-1}I_{1/2}{}^0(k^2) + 2y^{-3}(r'\cos\theta' - r\cos\theta)^2 I_{3/2}{}^0(k^2) \tag{A18}$$

$$G_{12}(r,r',\theta,\theta') = 2y^{-3}(r'\cos\theta' - r\cos\theta)[(r'\sin\theta' - r\sin\theta)I_{3/2}{}^0(k^2) - 2r'\sin\theta' I_{3/2}{}^1(k^2)]$$

$$G_{21}(r,r',\theta,\theta') = 2y^{-3}(r'\cos\theta' - r\cos\theta)[(r'\sin\theta' - r\sin\theta)I_{3/2}{}^0(k^2) + 2r\sin\theta I_{3/2}{}^1(k^2)]$$

$$G_{22}(r,r',\theta,\theta') = 2y^{-1}[I_{1/2}{}^0(k^2) - 2I_{1/2}{}^1(k^2)] + 2y^{-3}[(r'\sin\theta' - r\sin\theta)^2(I_{3/2}{}^0(k^2) - 2I_{3/2}{}^1(k^2)) - 4rr'\sin\theta\sin\theta' I_{3/2}{}^2(k^2)]$$

These integral equations can be discretized by breaking up the surface of the sphere into N angular patches and assuming $\mathbf{f}(\theta)$ is constant and equal to $\mathbf{f}_j$ for θ in the vicinity

$$y = (r^2 + r'^2 - 2rr'\cos(\theta - \theta'))^{1/2} \tag{A19}$$

$$k^2 = 4rr'\sin\theta\sin\theta'/y^2 \tag{A20}$$

$$I_{m/2}{}^n(k^2) = \int_0^\pi dx\, (1 + k^2\sin^2 x)^{-m/2}\sin^{2n} x \tag{A21}$$

of θ_j. Likewise, the fluid surrounding the sphere is broken up into M spherical shells as well as N angular patches, and it is assumed that $\mathbf{s}(r,\theta) = \mathbf{s}_{kj}$ for (r,θ) in the vicinity of (r_k,θ_j). Equations A14–A16 become

$$\mathbf{w}(r',\theta_i) = \sum_{j=1}^{N} \mathbf{E}_{ij} \cdot \mathbf{f}_j + \sum_{k=1}^{M}\sum_{j=1}^{N} \mathbf{H}_{ikj} \cdot \mathbf{s}_{ij} \qquad \text{(A22)}$$

where

$$\mathbf{E}_{ij} = \frac{a^2}{8\pi\eta}\int_{(j-1)\delta\theta}^{j\delta\theta} \sin\theta \, d\theta \, \mathbf{G}(a,r',\theta,\theta_i) \qquad \text{(A23)}$$

$$\mathbf{H}_{ikj} = \frac{1}{8\pi\eta}\int_{a+(k-1)\Delta r}^{a+k\delta r} r^2 \, dr \int_{(j-1)\delta\theta}^{j\delta\theta} \sin\theta \, d\theta \, \mathbf{G}(r,r',\theta,\theta_i) \qquad \text{(A24)}$$

$\Delta\theta = \pi/N$ radians and $\Delta r = (r^* - a)/(M - 1)$. In turn, r^* should be chosen sufficiently large that $\mathbf{s}_{Mj}$ makes a negligible contribution to eq A22. Choosing r^* such that $y_0(r^*)/y_0(a) = 10^{-4}$ insures this.

Equations A23 and 24 are evaluated numerically by successive approximation on higher resolution θ (or r and θ) lattices until the integrals converge to within a specified tolerance level, t.

$$|\mathrm{Tr}(\mathbf{E}_{ij}^{(s+1)} - \mathbf{E}_{ij}^{(s)})/\mathrm{Tr}(\mathbf{E}_{ij}^{(s+1)})| \le t \qquad \text{(A25)}$$

The velocity fields are independent of t for $t \ge 10^{-4}$. In this work t is set to 10^{-5}.

In addition to providing us a way of calculating the fluid velocity field, eq A22 is used to calculate $\mathbf{f}_i$. At the surface of the sphere, eq A22 becomes

$$\mathbf{w}_0 = \begin{pmatrix} -u \\ 0 \end{pmatrix} = \sum_{j=1}^{N} \mathbf{E}_{ij} \cdot \mathbf{f}_j + \sum_{k=1}^{M}\sum_{j=1}^{N} \mathbf{H}_{ikj} \cdot \mathbf{s}_{kj} \qquad \text{(A26)}$$

At the beginning of an iteration cycle, everything is known except $\{\mathbf{f}_j\}$. The superscript indicating iteration cycle is omitted for the sake of brevity. Let $\mathbf{E}_{ii}^{-1}$ denote the inverse of $\mathbf{E}_{ii}$; then

$$\mathbf{f}_i = \mathbf{E}_{ii}^{-1}\left[\mathbf{w}_0 - \sum_{j\neq i=1}^{N} \mathbf{E}_{ij} \cdot \mathbf{f}_j - \sum_{k=1}^{M}\sum_{j=1}^{N} \mathbf{H}_{ikj} \cdot \mathbf{s}_{kj}\right] \qquad \text{(A27)}$$

As in previous work, Gauss–Seidel iteration is used to solve for $\mathbf{f}_i$. One starts with an initial guess of all the $\mathbf{f}_i$'s, call if $\mathbf{f}_i^{(1)}$, and sequentially updates each element using current estimates of the other terms. Equation A27 becomes

$$\mathbf{f}_i^{(s+1)} = \mathbf{E}_{ii}^{-1}\left[\mathbf{w}_0 - \sum_{j=1}^{i-1} \mathbf{E}_{ij} \cdot \mathbf{f}_j^{(s+1)} - \sum_{j=i=1}^{N} \mathbf{E}_{ij} \cdot \mathbf{f}_j^{(s)} \sum_{k=1}^{M}\sum_{j=1}^{N} \mathbf{H}_{ikj} \cdot \mathbf{s}_{kj}\right] \qquad \text{(A28)}$$

where $s + 1$ denotes the update number. The procedure is repeated until the forces converge to some prespecified tolerance value, d, given by

$$d = \left[\sum_{j=1}^{N} (\mathbf{f}_j^{(s+1)} - \mathbf{f}_j^{(s)})^2 / \sum_{j=1}^{N} (\mathbf{f}_j^{(s+1)})^2\right]^{1/2} \qquad \text{(A29)}$$

In this work, d is set to 10^{-6}. Setting d to 10^{-8} results in no further change in the electrophoretic mobility to three significant figures. Once the $\mathbf{f}_i$'s are calculated, the hydrodynamic force on the polyion is given by (see eqs 4 and A10

$$z_{hl} = -2\pi a^2 \sum_{j=1}^{N} f_{j1}(\cos((j-1)\Delta\theta) - \cos(j\delta\theta)) \qquad \text{(A30)}$$

and $z_{h2} = 0$.

References and Notes

(1) Allison, S. A.; Nambi, P. *Macromolecules* **1992**, *25*, 3971.
(2) Lorentz, H. A. *Versl. Gewone Vergad. Afd. Natuurkd., K. Ned. Akad.* **1896**, *5*, 168.
(3) Odqvist, F. K. G. *Math. Z.* **1930**, *32*, 329.
(4) Ladyzhenskaya, O. A. *The Mathematical Theory of Viscous Incompressible Flow*, Gordon and Breach: New York, 1963; Chapter 3.
(5) Youngren, G. K.; Acrivos, A. *J. Fluid Mech.* **1975**, *69*, 377.
(6) Youngren, G. K.; Acrivos, A. *J. Chem. Phys.* **1975**, *63*, 3846.
(7) Henry, D. C. *Proc. R. Soc. London* **1931**, *A133*, 106.
(8) Overbeek, J. Th. G. *Adv. Colloid Sci.* **1950**, *3*, 97.
(9) Booth, F. *Proc. R. Soc. London* **1950**, *A203*, 514.
(10) Wiersema, P. H. On the Theory of Electrophoresis. Ph.D. Thesis, Utrecht University, Utrecht, The Netherlands, 1964.
(11) Wiersema, P. H.; Loeb, A. L.; Overbeek, J. Th. G. *J. Colloid Interface Sci.* **1966**, *22*, 78.
(12) O'Brien, R. W.; White, L. R. *J. Chem. Soc., Faraday Trans. 2* **1978**, *74*, 1607.
(13) Schellman, J. A.; Stigter, S. *Biopolymers* **1977**, *16*, 1415.
(14) Loeb, A. L.; Overbeek, J. Th. G.; Wiersema, P. H. *The Electric Double Layer Around a Spherical Colloid Particle*; MIT Press: Cambridge, MA, 1961.
(15) Warwicker, J.; Watson, H. C. *J. Mol. Biol.* **1982**, *157*, 671.
(16) Rogers, N. K.; Sternberg, M. J. E. *J. Mol. Biol.* **1984**, *174*, 527.
(17) Klapper, I.; Hagstrom, R.; Fine, R.; Sharp, K.; Honig, B. H. *Proteins* **1986**, *1*, 47.
(18) Jayaram, B.; Sharp, K. A.; Honig, B. *Biopolymers* **1989**, *28*, 975.
(19) Davis, M. E.; McCammon, J. A. *J. Comput. Chem.* **1989**, *10*, 386.
(20) Allison, S. A.; Sines, J. J.; Wierzbicki, A. *J. Phys. Chem.* **1989**, *93*, 5819.
(21) Sharp, K.; Fine, R.; Honig, B. H. *Science* **1987**, *236*, 1460.
(22) Allison, S. A.; Bacquet, R. J.; McCammon, J. A. *Biopolymers* **1988**, *27*, 251.
(23) Gilson, M. K.; Honig, B. H. *Nature* **1987**, *330*, 84.
(24) Gilson, M. K.; Davis, M. E.; Luty, B. A.; McCammon, J. A. *J. Phys. Chem.* **1993**, *97*, 3591.
(25) Becker, R. *Electromagnetic Fields and Interactions*; Blackie and Son: London, 1964.
(26) You, T. J.; Harvey, S. C. *J. Comput. Chem.* **1993**, *14*, 484.
(27) Zhou, H.-X. *Biophys. J.* **1993**, *65*, 955.
(28) Brandt, A. *Math. Comput.* **1977**, *31*, 333.
(29) Oberoi, H.; Allewell, N. M. *Biophys. J.* **1993**, *65*, 48.
(30) Kim, S.; Karrila, S. J. *Microhydrodynamics*; Butterworth-Heinemann: Boston, 1991.
(31) Brune, D.; Kim, S. *Proc. Natl. Acad. Sci. U.S.A.* **1993**, *90*, 3835.
(32) Stigter, D. *J. Phys. Chem.* **1978**, *82*, 1417, 1424.
(33) Fixman, M. *Macromolecules* **1980**, *13*, 711.
(34) Derjaguin, B. V.; Dukhin, S. S.; Shilov, V. N. *Adv. Colloid Interface Sci.* **1980**, *13*, 141.
(35) Dukhin, S. S.; Shilov, V. N. *Adv. Colloid Interface Sci.* **1980**, *13*, 153.